Modeling of Multiscale and Multiphase Phenomena in Materials Processing

ANDREAS LUDWIG, ABDELLAH KHARICHA, and MENGHUAI WU

In order to demonstrate how CFD can help scientists and engineers to better understand the fundamentals of engineering processes, a number of examples are shown and discussed. The paper covers (i) special aspects of continuous casting of steel including turbulence, motion and entrapment of non-metallic inclusions, and impact of soft reduction; (ii) multiple flow phenomena and multiscale aspects during casting of large ingots including flow-induced columnar-to-equiaxed transition and 3D formation of channel segregation; (iii) multiphase magneto-hydrodynamics during electro-slag remelting; and (iv) melt flow and solidification of thin but large centrifugal castings.

DOI: 10.1007/s11663-013-9820-1

I. INTRODUCTION

SINCE the Bronze and the Iron Ages, materials processing, and here especially metallurgy, has held a global importance for the economic well-being of societies. It is thus understandable that metallurgy has changed from arts and crafts into an engineering specialty, where the knowledge of centuries has led to an enormous commercial and technical efficiency. However, increasing competition and the necessitation of energy- and CO_2-reduced manufacturing methods require the improvement of existing techniques and even the development of new, alternative production technologies. On the other hand, the opacity of liquid and solid materials and the involved high temperatures make the experimental penetration of metallurgical processes, and with that the attainment of detailed process knowledge, quite difficult.

Here, numerical process simulations put us in a position to zoom into process details and learn more about procedures that happen inside the product during its production. For around four decades, numerical descriptions of nearly all production processes have come up and with time, the impression is conveyed that nowadays the existing simulation tools are able to answer nearly all our questions. However, people who are dealing with computer simulations everyday know that the forecast ability of a numerical tool depends highly on the underlying physical model. If a certain phenomenon is not described properly in the program, the numerical tool cannot give sound predictions on its consequences. Therefore, it is important to know the origin of the observation made in praxis and to create model descriptions capturing the involved physics.

ANDREAS LUDWIG, Professor, ABDELLAH KHARICHA, Senior Lecturer, and MENGHUAI WU, Associate Professor, are with the Department Metallurgy, University of Leoben, Franz-Josef-Strasse 18, 8200, Leoben, Austria. Contact e-mail: ludwig@unileoben.ac.at
Manuscript submitted May 1, 2012.
Article published online March 20, 2013.

In the present paper, we will take a look at four different metallurgical processes and discuss the present edge of ability of its numerical simulation, namely (i) Continuous and DC casting, (ii) ingot casting, (iii) electro-slag remelting, and (iv) centrifugal casting. We apologize for not being able to quote all groups who have contributed to the state of the art. The fact that the field is not easy to survey becomes obvious by taking a look at the program of the Int. Conf. METEC-InSteelCon 2011 which is composed of four different international conferences relevant to steelmaking,[1] not to mention of corresponding conferences for Cu- and Al-based alloys or other alloys.

II. MODELING EXAMPLES

A. *Aspects of Continuous and DC Casting*

After secondary metallurgical treatment in different aggregates (*e.g.*, VD, VOD, AOD, and RH), the liquid metal is poured from the ladle into the tundish, from where it flows through the submerged entry nozzle into the casting mold. Here, it starts to solidify most often in the form of equiaxed and columnar dendritic crystals. During solidification and due to intensive cooling, the strand (billet, bloom, or slab) contracts. The interplay of mechanical guidance, thermal contraction, and metallostatic pressure leads to the typical deformation history which might often lead to unacceptable quality problems.

All of the process steps mentioned above are nowadays subject to numerical simulation, whereby pure flow simulation even when turbulence and temperature changes are considered must be seen as standard. Challenging topics arise when different phenomena interact as

(a) liquid metal flow and gas bubble motion especially in turbulent regimes;
(b) formation and motion of non-metallic inclusions and their interplay with refractory materials, gas

bubbles, turbulent eddies, and entrapment/engulfment into the solidifying shell;
(c) flow and solidification, especially interdendritic flow and turbulence damping;
(d) microstructure formation and its dependence on grain motion and melt flow;
(e) natural buoyancy caused by cooling and solidification-induced compositional heterogeneity (segregation);
(f) flow, solidification, and deformation which might cause the occurrence of hot cracking;
(g) creep and viscoplastic material behavior in the two-phase region.

Most advance research groups are currently working on the topics listed above,[2–32] whereby very often model formulations for a simple academic case are suggested where measurements on an idealized system might exist. However, the application to real and complex industrial situations is much more challenging and fails often due to the lack of reasonable materials' properties (as interface tensions, solutal expansion coefficients, melt viscosities especially in mushy regions, *etc*.) or unknown intrinsic process details (as permeability of dendritic mushy zones, solid fraction evolution in the presence of local melt flow, *etc*.). Also, available computer resources are often a hindrance to the application of suitable models to real process applications.

An example of a process where turbulent melt flow, dendritic solidification, and local contraction and deformation interact is thin slab casting of steel (Figure 1). In standard continuous casting of steel, the turbulent melt flow from the SEN into the mold region is quite separated from the formation of the solid shell. Even isothermal flow studies of mold regions are often thought to represent the industrial reality and so water models are used to get experimental details. However, sophisticated modeling approaches have demonstrated that the existence of the solidifying shell may change the overall flow pattern in the mold region.[6] In the quoted work, it was also shown that Argon gas, which might be used to constantly purge the SEN and thus to prevent clogging, may also affect the flow pattern in the mold region.

When it comes to the description of the interaction between turbulent melt flow and dendritic solidification, it has to be stated that no physically sound model has been suggested yet. Although the importance of melt flow for the formation of a dendritic mushy zone has been outlined,[18] only oversimplified approaches are in use.[19] A similar statement must be made for the description of dendritic solidification and particle entrapment during continuous casting of steel.[20–23] Although turbulent particle dispersion in the mold region is accounted for[6] and a force balance at the dendrite tips decides on particle pushing or engulfment, the results are still questionable.[20] The reason for necessary skepticism is the fact that the largest force in the model might exist for liquid inclusions only and not for the much more common solid inclusions.

Another example for a complex interaction of different phenomena is the occurrence of centerline segregation in steel strands. While a strand solidifies from outside inward, its core remains liquid or at least mushy for quite a long time. As thermal and solidification-induced shrinkage has to be compensated by feeding with melt and as metallostatic pressure leads to bulging of the solidified outer shell, complex flow phenomena inside the strand lead to a macroscopic redistribution of alloying elements. In order to describe this phenomenon, shell mechanics have to be combined with two-phase flow descriptions inside the solidifying strand core. For this topic, only simplifying descriptions exist. The authors' group studied the shrinkage flow-induced macrosegregation in continuous casting of steel without considering shell bulging.[24] They predicted negative centerline segregation. Then, in a series of publications, it was demonstrated that by considering both shrinkage-induced feeding flow and bulging-induced core flow, the centerline segregation will become positive.[25–29] Figure 2 shows how the local flow field in the two-phase core of the solidifying stand may result in the formation of positive centerline segregation.[30–32] In Reference 32 how mechanical soft reduction might be usable to reduce positive centerline segregation is discussed.

In DC casting of Cu- or Al-based alloys, advanced simulation efforts focus on the prediction of macrosegregation in ternary systems for purely columnar solidifying strands.[33–38] The formation of macrosegregation in the mixed columnar and equiaxed solidifying case is still subject to future challenges. Another interesting fluid–structure interaction-type topic is the interaction of a flexible combo bag with the flow in a DC Aluminum Casting.[39]

B. *Aspects of Big Ingot Casting*

Although most steel products are nowadays produced with continuous casting processes, large steel ingots are still required for manufacturing electric power plant turbine shafts, generator rotor shafts, nuclear pressure vessels, chemical pressure vessels, ship parts, and other heavy machinery parts. The knowledge for producing steel ingots was mainly gained in the last century,[40–44] but the problems which haunted foundry men for decades were still not solved, even not fully understood. They are as follows:

(a) formation of A- and V-macrosegregation;
(b) formation of the typical as-cast structure (columnar-to-equiaxed transition: CET);
(c) motion and engulfment of non-metallic inclusions;
(d) occurrence of hot tearing in extremely large ingots; *etc*.

The cost of full-scale trials was so high that people had to think of developing theoretic models of the formation of segregations in ingots.[42–45] Therefore, a series of modeling activities was carried out in the authors' group. A 3-phase model was developed for mixed columnar-equiaxed solidification in ingot casting.[46,47] A volume averaging concept was taken to allow the modeling approach to be applicable for the solidification of ingot casting at the process scale.[47–50] Thermodynamics was coupled with the solidification

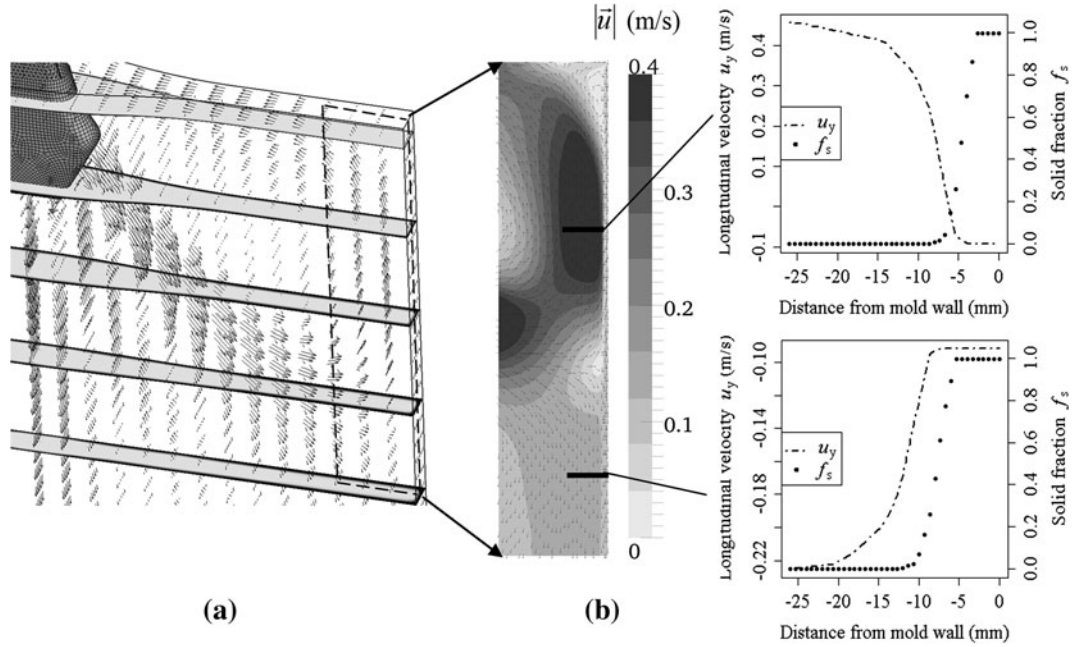

Fig. 1—Quasi steady state simulation result of an engineering thin slap casting (width 1726 mm and thickness 72 mm): (*a*) 3D distribution of the velocity vector field and evolution of the solid shell; (*b*) zoomed velocity field in the central plane near the narrow face; (*c*) detailed velocity (u_y component) profile and solid volume fraction along two paths across the mushy zone (taken from Ref. [22]).

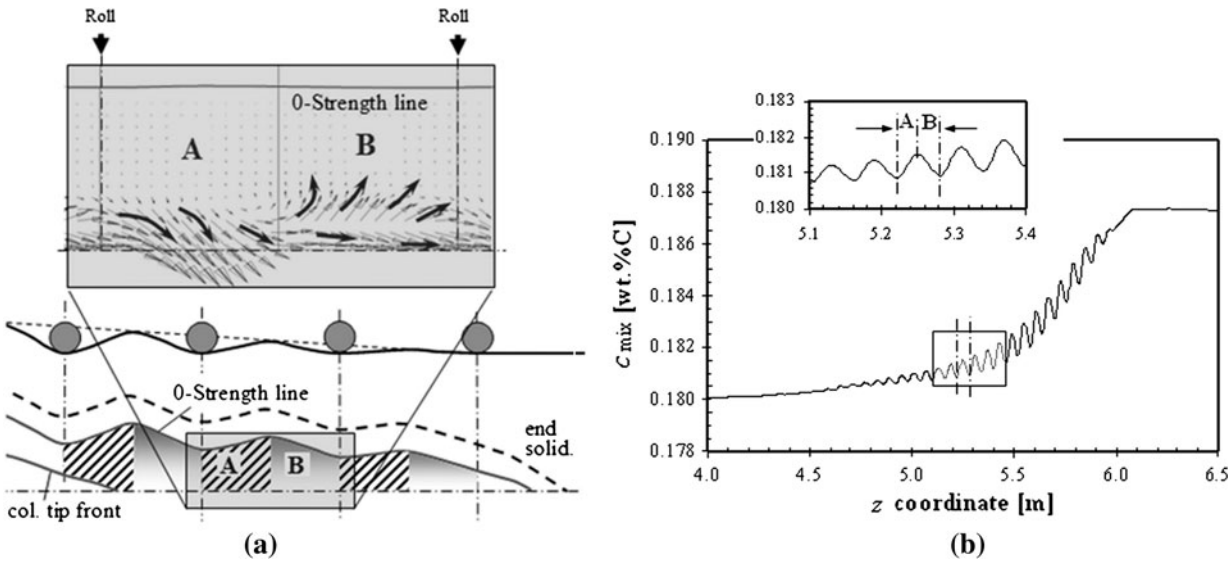

Fig. 2—Local flow field in the two-phase core of a solidifying steel strand and the resulting formation of positive centerline segregation (taken from Ref. [30]).

kinetics to consider the multicomponent alloy system.[51–64] Very recently, the dendritic, multiscale nature of the solidifying crystals was also taken into account in the model.[65–70] In the meantime, the modeling approach was applied to study the formation mechanism of macrosegregation[71] and the as-cast structure including CET.[72]

An example of a 3-phase modeling result of a laboratory benchmark ingot (ϕ 66 mm × 170 mm) is given in Figure 3. Details about the settings for this benchmark refer to previous publications.[46,47,64] It shows the solidification sequence, including sedimentation of the globular equiaxed grains, the sedimentation-induced, and thermo-solutal buoyancy-induced melt convection. The columnar dendrites grow from the mold wall and the columnar tip front moves inward. The equiaxed grains nucleate near the mold walls and in the bulk melt. The columnar dendrites are stationary, whereas the equiaxed grains sink and settle in the base of the ingot. The accumulation of such grains at the base of the ingot has a characteristic cone shape. The sedimentation of grains and the melt convection influence the

macroscopic solidification sequence and thus the final phase distribution. More equiaxed grains will be found at the bottom and in the base region, while columnar solidification will be predominant in the upper part of the ingot. As the columnar tip front is explicitly tracked, the simulation shows that the columnar tip fronts from both sides tend to meet in the casting center. However, in the lower part of the casting, the large amount of equiaxed grains stops the propagation of the columnar tip front. Its final position indicates the CET position. The CET separates areas where only equiaxed grains appear from areas where both columnar dendrites and equiaxed grains might occur side by side. The above benchmark simulation was not directly evaluated against experimental results as ideal non-dendritic crystal morphology and some process parameters were assumed. But, the key features of the mixed columnar-equiaxed solidification in steel ingot were proven to be reproducible numerically. The solidification dynamics as described above fit with the widely accepted explanations of experimental findings as summarized by Campbell:[55] "The fragments (equiaxed grains) fall at a rate somewhere between that of a stone and snow. They are likely to grow as they fall if they travel through the undercooled liquid just ahead of the growing columnar front, possibly by rolling or tumbling down this front. The heap of such grains at the base of the ingot has a characteristic cone shape."

A two-phase columnar solidification model was used to study the formation mechanism of the channel segregation in a Sn-10 wt pct Pb benchmark ingot, as shown in Figure 4. The size of the benchmark is $50 \times 60 \times 30$ mm^3. Details of alloy and process parameters were defined by Bellet *et al.*[56]The two phases considered in the current model are the melt and columnar phase. Transient development of flow channels during solidification can be numerically "visualized." The iso-surface of liquid volume fraction $f_\ell = 0.35$ is plotted and reveals the 3D nature of the channels. They are discontinuous, lamellar structured, and originate from the region adjacent to the cooling wall, from which they develop with a certain angle

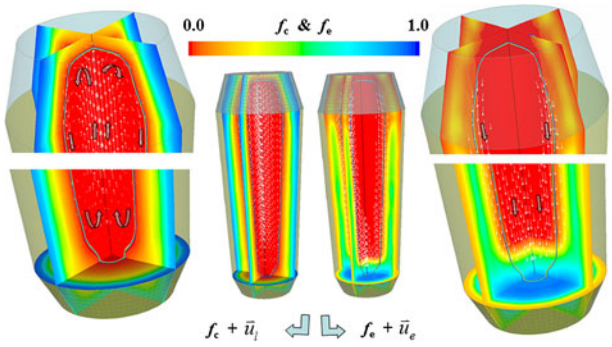

Fig. 3—Schematic of the solidification sequence of a laboratory benchmark ingot.[46,47,64] The volume fraction of the columnar and equiaxed phases, f_c and f_e, are shown in color in two vertical and one horizontal sections, the velocity fields of the liquid melt and the settling equiaxed grains, $\vec{u}_l$ and $\vec{u}_e$, are shown as vectors. The maximum velocity of liquid melt can reach 17 mm/s and the maximum velocity of the settling equiaxed crystals can reach 24 mm/s. The columnar tip front position is also shown by iso-surfaces.

(about 40–60 deg to the horizontal plane). The channel spacing (distance between neighboring channels) is almost constant or slightly adjusted with time during solidification. It is verified by the current model that remelting is not a necessary condition for the formation of channel segregation. Although remelting is not included in the current simulation benchmark, the channel segregation still appears. Verification of the current model was made by a comparison with other modeling approaches[57–60] and with the experiments of Hebditch and Hunt.[61]

C. *Aspects of Electro-Slag Remelting*

In the past few years, remelting technologies have taken an important role in the large field of special materials, and the number of Electro-Slag Remelting (ESR) and Vacuum Arc Remelting (VAR) units is continuing to grow. In the ESR process, an as-cast electrode is immersed into a hot slag such that droplets depart from the melting electrode, pass through the turbulently flowing slag, and finally feed a liquid metal pool which then solidifies directionally. Hereby, a high electric current heats up the slag by Joule heating. In the VAR process, the gap between the electrode and the pool is put under metallurgical vacuum and the high current creates one arc or several arcs between the electrode and the pool, which then cause a continuous melt flow to occur. Nowadays, ESR and VAR are commonly in use. However, far-reaching investigations on an industrial scale in particular have rarely been published. There is still a great demand for more knowledge on these processes and how to optimize them for several alloys qualities, melting parameters, and ingot sizes. To produce a high quality homogeneous ingot with good surface quality, the deviations in the process, such as melting rate or the immersion depth of the electrode, need to be minimized.

During the process, the electric parameters such as current, voltage, and electric resistance are continuously recorded. The variation of the resistance, known as resistance swing, is often used for the control of the electrode position.[73] A higher level of resistance swing is interpreted as a low electrode immersion depth. However, the increase in resistance swing can be reliably, but not quantitatively, related with the immersion depth. This is why some effort must be made for the identification of the process state, solely through analysis of electric process parameters. To achieve this goal, it is important to identify the phenomena that can generate these electric fluctuations. Assuming that most of the resistance is generated within the slag cap, the analysis focused on the possible paths that the electric current can take through this region. The slag region experiences strong flow turbulence that can induce locally strong temperature fluctuations. Large and fast fluctuations of the resistance can only be generated by modifying the shape of the slag cap. The solid slag that develops at the mold (referred as slag skin) is a boundary that was considered for a long time as an electric insulator.[74,75] Recent experimental and numerical investigations on static mold ESR have shown that

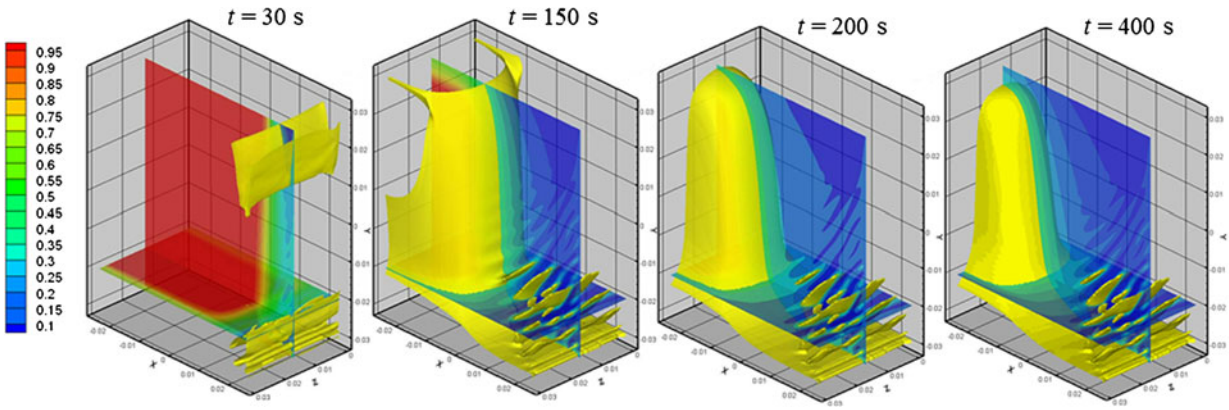

Fig. 4—Predicted 3D solidification sequence in a Sn-10 wt pct Pb benchmark ingot, from (*a*) 30 s to (*d*) 400 s. The liquid volume fraction in two planes (a vertical central plane and a horizontal plane with a distance of 0.01 m from the bottom) is shown using a color scale. In addition, the iso-surface of liquid volume fraction $f_\ell = 0.35$ is shown to demonstrate the formation sequence of flow channels.

typically 20 pct (but up to 80 pct) of the total current can cross the solid slag layer to enter directly into the mold.[76,77] The ratio mold current over the vertical current depends on two factors: first, on the ratio between the electrode-mold radial distance and the slag cap height and, second, on the ratio between liquid slag and slag skin electric conductivities.

From a fluid dynamic point of view, the ESR process is clearly a multiphase process, with free interfaces (slag/pool, gas/slag) and with a mixed area (slag and falling steel droplets).[76–84] As the electric conductivity of the metal is known to be much higher than that of the slag, the distribution of the metallic phase within the slag is a critical parameter to predict the distribution of the electric current density which in turn controls the Lorentz force magnitude. From these physical facts, one can expect that in this nonlinear system, a slight change in the position of the interfaces in the slag can result in totally different flow behavior. Physically, the development of the heat and mass transfer at the interfaces is important for the final ingot quality, composition, and cleanliness. Unfortunately, a visual observation of the droplet formation and interface movement is almost impossible.

To explore the process numerically, it is necessary to model the strong coupling between the flow and the electrodynamic phenomena. This typical magnetohydrodynamical problem was tackled with the help of a 3D MHD-VOF model which is able to predict the electric and magnetic field distribution in function of the metallic distribution in the low electric conductivity slag. As shown in Figures 5 and 6, it is nowadays possible to virtually see the melting phenomena for small- and even for large-scale ESR process. On a small scale, the droplet formation occurs only at the center. At a larger scale, the liquid film that develops under the electrode allows droplet departure from many different positions. The way that the liquid metal droplets enter the liquid pool is one major factor which determines the liquid pool shape and depth. The reason why the dripping occurs in the middle on a small scale lies in the ratio between the Lorentz force and the buoyancy forces. The Lorentz force acts mainly in the inward direction toward the center, while buoyancy results in a flow which is outward toward the mold. The Lorentz force being larger in small ESR, the liquid metal film under the electrode has the tendency to accumulate at the center of the electrode. At a larger scale, the Lorentz force is not strong enough to oppose the turbulent movement of the hot slag under the electrode. However, the combined effects of the droplets' impacts and the Lorentz force are strong enough to generate a three-dimensional wavy movement of the slag/pool interface. This movement generates a strong 3D movement of the flow not only in the liquid pool but also in the slag. This 3D movement was clearly observed on the surface of the exposed slag in an industrial plant. Models that use 2D axisymmetric approximation can only predict radially inward or outward motion at the exposed slag surface.[73–75] This first success in modeling is only a first step toward the full understanding of the multiphysics phenomena that occur in this process. In the future, the following questions need to be investigated:

(a) How axisymmetric is the system, especially the electric current and liquid flow? How does the symmetry affect the solidification? In previous 3D investigations, the current was not allowed to cross the solid slag skin. Thus, how will the system behave if the current is left free? A breaking of the global axial symmetry of the current path might occur at the lateral mold wall;
(b) Mechanisms of removal of non-metallic inclusion. How important are the effects of the electromagnetic Lorentz force?
(c) Melting tip of the electrode, flat, or conical depends on the exact thermal and hydrodynamic conditions occurring in the slag;
(d) Development and evolution of the liquid film under the electrode and how it is related to the droplet transfer to the liquid pool;
(e) Formation of the solid shell just under the slag/pool interface, which can generate bad ingot surface quality.

D. *Aspects of Centrifugal Casting*

The horizontal spin casting process (HSC) is a casting process that generally has several advantages above a

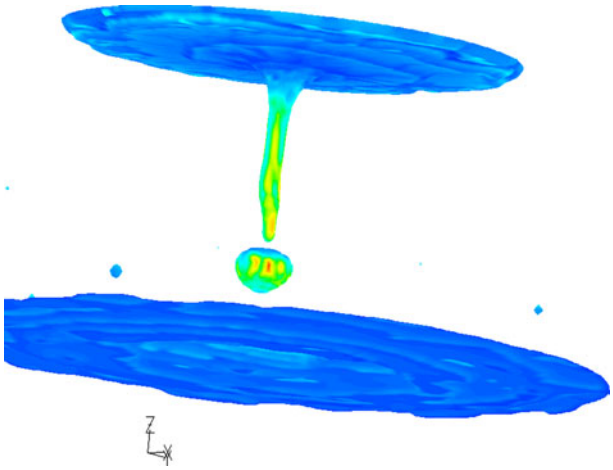

Fig. 5—Electric current density in a small-scale ESR (20 cm diameter) color scaled from blue to red (10^5 to 10^9 Amps/m^2) over the slag/metal interface. A current of 3000 Amps is passed through an electrode of 13 cm diameter (top surface). The current flows through the metallic faucet and through the detached droplet. The latest fall and impact on the slag/liquid pool interface (bottom surface). Note that the slag phase has been faded out.

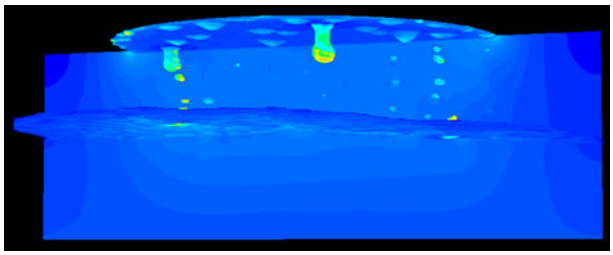

Fig. 6—Electric current density in a large-scale ESR (diameter 52 cm). A current of 13000 Amps is passed through an electrode of now 42 cm diameter (top surface).[84] The metal/slag interface and a vertical section are colored according to the electric current density, scaled from blue to red (10^4 to 10^8 Amps/m^2). Several faucets and liquid droplets are visible in the slag region (being faded out). Notice the deformation of the slag/metal pool interface (bottom surface).

traditional gravity casting process and also some other casting processes. The main profit is usually superior mechanical properties.[85–93] Centrifugally cast products have a high degree of metallurgical purity and homogeneous microstructure. A significant gain is observed for the rupture strength, the rupture strain, and for the Young modulus. These properties naturally depend on the centrifugal force and thus, the higher the distance from the rotation center, the better the increase in mechanical properties.

Since the centrifugal force is defined as the product of the radius and the square of the angular frequency, the final mechanical properties mostly depend on the selection of the angular frequency. The proper selection of the angular frequency has to be done in order to prevent so-called raining on the one hand, *i.e.*, metal droplets can fall down from the upper part of the inside surface of the casting product due to the low centrifugal acceleration and the winning counteracting action of the gravity. On the other hand, excessive speeds can lead to the longitudinal cracks caused by the hoop stress in the initially solidified layer.

During horizontal spin casting of rolls, vibrations and mold deformations seem to have a significant effect on the final quality of the product.[85,86] There are several physical sources of vibrations that can be found. First, it is a poor roundness and a static imbalance of the chill itself. Secondly, those are free vibrations linked with natural frequencies of the rotating mold being subject to strong thermomechanical deformation and to combined action of the centrifugal and Coriolis stresses.

In order to explore those effects, a 2D shallow layer model was built by the authors to simulate the hydrodynamic behavior of a liquid metal layer over an inner surface of a rotating cylinder. This approach differs sensitively from the ones typically used to simulate this process. Usually, the flow in a centrifugal configuration is solved in 3D.[87–90] Due to the convective limitation in the Courant number, 3D approaches need an extremely small time step if accurate calculations are targeted. The shallow layer approach can be an interesting alternative to the 3D approach if the thickness of the liquid film is smaller than the mold radius. In the present model, a parabolic velocity profile is assumed with maximum velocity on the free surface and zero velocity on the wall. Due to a high angular frequency Ω, the liquid is mainly rotating with the mold; therefore, the model is defined in the rotating frame of reference. We introduce sine-like vibrations in the radial and tangential directions generated by a small default roundness of the mold. The possible occurrence of the bending of the mold axis is also considered. The introduction of bending and vibrations in the model induces a strong modification in the mathematical expression of the fictitious forces such as the centrifugal and the Coriolis forces. As opposed to a perfectly round and aligned mold, these forces are position and time dependent. They are able to generate unexpected flow movements and waves. Typical liquid flow velocities (relative to the rotating mold) reach values as large as 1 m/s. The wave dynamic was found to be very complex (Figure 7); it can take up to a minute before the bifurcation of the system to a steady chaotic state occurs. Although the vibrations were assumed to act only in the radial and tangential directions, the system gave rise to waves mainly propagating in the axial direction. The origin of this phenomenon is probably related to the rotational property of the Coriolis force; the latest redirects the kinetic energy in a perpendicular direction. The velocity magnitude generated by these vibrations is strong enough to be able to fragment and transport relatively large solidified crystals far from the region where they originally nucleated.[91]

In the future, the 3 shallow layers approach will be used to simulate the solidification process. It will include the liquid region, a semi-liquid semi-solid granular layer, and a totally solidified layer. The equations of heat transfer and phase change and the equation motion of the granular region will be added to the present model.

III. CONCLUSIONS

In material processing, numerical modeling tools are more and more in use. Temperature and flow field

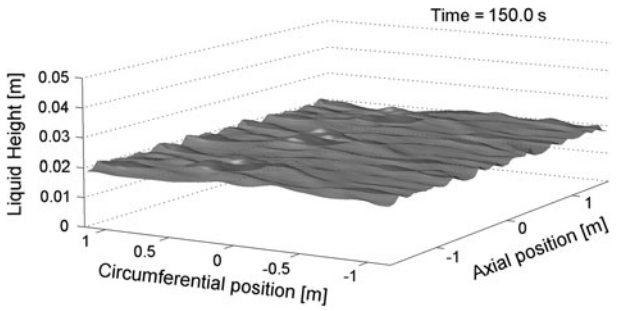

Fig. 7—Waves at the metal/air interface during the developed flow regime generated by the action of the centrifugal force, Coriolis force, gravity, friction, and vibrations. The mold is 3.2 m long with the inner mold radius of 0.372 m. The average liquid height is 20 mm; the mold is rotating at a rotating speed of 30 rad/s.

predictions are nowadays quite reliable. However, the multiphase and multiscale nature of many industrial processes often limits the predictive efficiency even of the most sophisticated programs. With the help of four examples, we have demonstrated that sound predictions of important process details are only possible if the involved physics is modeled adequately. Especially when different phenomena interact, *e.g.*, flow, solidification, and stress-induced deformations or motion of a dendritic crystal in a turbulent melt flow, our knowledge is still limited. Nowadays, it is true that a successful extension of a numerical code is quite often accompanied by an increase of knowledge about important process details and *vice versa*.

ACKNOWLEDGMENTS

The authors are grateful for financial support over the years by Böhler Edelstahl, RHI Technologies, Siemens-VAI, Voestalpine Stahl Donawitz, Voestalpine Stahl Linz, and the public agencies the Christian-Doppler Society and FFG. We also acknowledge contributions from present and former staff members Bohacek, Domitner, Eck, Grasser (formerly Gruber-Pretzler), Hao, Ishmurzin, Könözy, Li, Mayer, Nunner, Pfeiler, and Vakhrushev.

REFERENCES

1. www.metec-insteelcon2011.com/files/pdfs/Metec_Session_Programme.pdf.
2. B.G. Thomas: *59th Electric Furnace Conference, Pheonix, AZ,* Iron & Steel Soc., 2001, pp. 3–30.
3. B.G. Thomas: *Modeling for Casting and Solidification Processes*, K.-O. Yu, ed., Marcel Dekker Inc., New York, 2002, pp. 499–540.
4. B.G. Thomas, Q. Yuan, B. Zhao, and S. Vanka: *JOM-e.*, 2006, vol. 58, pp. 16–18.
5. S. Koric, L.C. Hibbeler, and B.G. Thomas: *Int. J. Numer. Meth. Eng.*, 2009, vol. 78, pp. 1–31.
6. Q. Yuan and B.G. Thomas: *3rd International Congress on Science and Technology of Steelmaking*, Charlotte/NC, AISTech, Warrendale, PA, 2005, pp. 745–62.
7. A. Ramos-Banderas, R. Sanchez-Perez, R.D. Morales, J. Palofox, and L. Garcia-Demedices: *Metall. Mater. Trans. B*, 2004, vol. 35B, pp. 449–60.
8. Q. Yuan, B.G. Thomas, and S.P. Vanka: *Metall. Mater. Trans. B*, 2004, vol. 35B, pp. 685–702.
9. Q. Yuan, B.G. Thomas, and S.P. Vanka: *Metall. Mater. Trans. B*, 2004, vol. 35B, pp. 703–14.
10. D. Mazumdar and R.I.L. Guthrie: *Metall. Mater. Trans. B*, 1994, vol. 25B, pp. 308–12.
11. A. Mukhopadhyay, E.W. Grald, K. Dhanasekharan, S. Sarkar, and J. Sanyal: *Steel Res. Int.*, 2005, vol. 76, pp. 22–32.
12. M.P. Schwarz: *Appl. Math. Modell.*, 1996, vol. 20, pp. 41–51.
13. A. Alexiadis, P. Gardin, and J.F. Domgin: *Metall. Mater. Trans. B*, 2004, vol. 35B, pp. 949–56.
14. J.E. Camporredondo, A.H. Castillejos, F.A. Acosta, E.P. Gutierrez, and M.A. Herrera: *Metall. Mater. Trans. B*, 2004, vol. 35B, pp. 541–60.
15. K. Cukierski and B.G. Thomas: *Metall. Mater. Trans. B*, 2008, vol. 39B, pp. 94–107.
16. H. Liu, C. Yang, H. Zhang, Q. Zhai, and Y. Gan: *ISIJ Int.*, 2011, vol. 51, pp. 392–401.
17. C. Pfeiler: Ph.D. Thesis, University of Leoben, 2008.
18. M. Wu, A. Vakhrushev, G. Nunner, C. Pfeiler, A. Kharicha, and A. Ludwig: *Open Transp. Phenomena J.*, 2010, vol. 2, pp. 16–23.
19. A. Vakhrushev, A. Ludwig, M. Wu, Y. Tang, G. Nitzl, and G. Hackl: *4rd International Conference on Simulation and Modeling in Metallurgical Processes in Steelmaking*, Düsseldorf, Germany, 2011, pp. 17.1–8.
20. C. Pfeiler, B.G. Thomas, M. Wu, A. Ludwig, and A. Kharicha: *Steel Res. Int.*, 2008, vol. 79, pp. 599–607.
21. C. Pfeiler, B.G. Thomas, A. Ludwig, and M. Wu: *2nd International Conference on Simulation and Modeling in Metallurgical Processes in Steelmaking*, A. Ludwig, ed., Graz, Austria, 2007, pp. 247–52.
22. A. Vakhrushev, A. Ludwig, M. Wu, Y. Tang, G. Nitzl, and G. Hackl: *European Continuous Casting Conference*, Düsseldorf, Germany, 2011, pp. 18.1–10.
23. A. Vakhrushev, M. Wu, A. Ludwig, Y. Tang, G. Hackl, and G. Nitzl: *13th International Conference Modeling of Casting, Welding and Advanced Solidification Processes*, A. Ludwig, M. Wu, A. Kharicha, eds., Schladming, Austria, *IOP Conf. Series: Mater. Sci. Eng.*, 2012, DOI:10.1088/1757-899X/33/1/012014.
24. F. Mayer, M. Gruber-Pretzler, M. Wu, and A. Ludwig: *2nd International Conference on Simulation and Modeling in Metallurgical Processes in Steelmaking*, A. Ludwig, ed., Graz, Austria, 2007, pp. 265–70.
25. F. Mayer, M. Wu, and A. Ludwig: *12th International Conference on Modeling of Casting, Welding and Advanced Solidification Processes*, S.L. Cockcroft *et al.*, eds., Vancouver, Canada, 2009, pp. 279–86.
26. F. Mayer, M. Wu and A. Ludwig: *3rd International Conference of Simulation and Modeling in Metallurgical Processes in Steelmaking*, Leoben, Austria, Ed. A. Ludwig, 2009, pp. 247–52.
27. F. Mayer, M. Wu, and A. Ludwig: *Steel Res. Int.*, 2010, vol. 81, pp. 660–67.
28. M. Wu, A. Ludwig, C. Pfeiler and F. Mayer: *4th International Conference on Continuous Casting of Steel in Developing Countries*, Beijing, China, 2008, pp. 30–37.
29. M. Wu, A. Ludwig, C. Pfeiler, and F. Mayer: *J. Iron Steel Res. Int.*, 2008, vol. 15, pp. 30–37.
30. M. Wu, J. Domitner, A. Ludwig and F. Mayer: *4th International Conference on Simulation and Modeling in Metallurgical Processes in Steelmaking*, Düsseldorf, Germany, 2011, pp. S4.1–11.
31. J. Domitner, M. Wu, F. Mayer, A. Ludwig, B. Kaufmann, J. Reiter, and T. Schaden: *7th European Continuous Casting Conference*, Düsseldorf, Germany, 2011, pp. S6.1–8.
32. M. Wu, J. Domitner, and A. Ludwig: *Metall. Mater. Trans. A*, 2012, vol. 43A, pp. 945–64.
33. M. Gruber-Pretzler, M. Wu, A. Ludwig, J. Riedle and U. Hofmann: *International Conference COM/Cu2007*, Canada, J. Hugens, K. Sadayappan, J. Spooner, L.D. Smith, C. Teigge-Molecey, J. Kapusta, A. Fuwa, N. Piret, eds., Canadian Inst. Mining, Metall. Petroleum, 2007, pp. 265–79.
34. M. Gruber-Pretzler: Ph.D. Thesis, University of Leoben, Austria, 2008.
35. M. Grasser, A. Ishmurzin, F. Mayer, M. Wu, A. Ludwig, U. Hofmann and J. Riedle: *12th International Conference on Modeling Of Casting, Welding, and Advanced Solidification Processes*, S.L. Cockcroft *et al.*, eds., Vancouver, Canada, 2009, pp. 221–28.
36. A. Eck, C. Pfeiler, A. Kharicha, A. Ludwig, and J.W. Evans: *TMS Annual Meeting, Proceedings. Book "Materials Processing Fundamentals"*, 2009, pp. 221–8.

37. J. Hao, M. Grasser, A. Ishmurzin, M. Wu, A. Ludwig, J. Riedle, and R. Eberle: *Inernational Conference Copper 2010*, Hamburg, Germany, 2010, pp. 65–80.
38. J. Hao, M. Grasser, M. Wu, and A. Ludwig: *Adv. Mater. Res*, 2011, vols. 154–155, pp. 1401–04.
39. A. Kharicha, A. Ludwig, and M. Wu: *DGM Symposium Stranggiessen 2010*, ed. H.R. Müller, Werkstoffinformationsgesellschaft Frankfurt, 2010, supplement.
40. Iron and Steel Institute (London): "Report on the heterogeneity of steel ingots", *J. Iron Steel Inst*., 1926, vol. 10, p. 39.
41. J.J. Moore and N.A. Shah: *Int. Metals Rev*., 1983, vol. 28, pp. 338–56.
42. M.C. Flemings: *ISIJ Int*., 2000, vol. 40, pp. 833–41.
43. C. Beckermann: *Int. Mater. Rev*., 2002, vol. 47, pp. 243–61.
44. G. Lesoult: *Mater. Sci. Eng. A*, 2005, vols. 413–414, pp. 19–29.
45. H. Combeau, M. Zaloznik, S. Hand, and P.E. Richy: *Metall. Mater. Trans. B*, 2009, vol. 40B, pp. 289–304.
46. M. Wu and A. Ludwig: *Metall. Mater. Trans. A*, 2006, vol. 37A, pp. 1613–31.
47. M. Wu and A. Ludwig: *Metall. Mater. Trans. A*, 2007, vol. 38A, pp. 1465–75.
48. M. Wu and A. Ludwig: *11th International Conference on Modeling of Casting, Welding and Advanced Solidification Processes* , C.A. Gandin *et al*., eds., Opio, France, 2006, pp. 291–98.
49. M. Wu, L. Könözsy, A. Fjeld, and A. Ludwig: *7th Pacific Rim International Conference on Modeling of Casting & Solidification Processes*, J.Z. Jin, S. Yao, H. Hao, T.M. Wang, eds., Dalian, China, 2007, pp. 379–87.
50. M. Wu, L. Könözsy, A. Fjeld, and A. Ludwig: *2nd International Conference on Simulation and Modeling in Metallurgical Processes in Steelmaking*, Graz, Austria, Ed. A. Ludwig, 2007, pp. 114–19.
51. A. Ishmurzin, M. Gruber-Pretzler, F. Mayer, M. Wu, and A. Ludwig: *Int. J. Mat. Res*., 2008, vol. 99, pp. 618–25.
52. A. Ludwig, A. Ishmurzin, M. Gruber-Pretzler, F. Mayer, M. Wu, R. Tanzer, and W. Schützenhöfer: *5th December International Conference on Solidification Processing*, H. Jones, ed., Sheffield, UK, 2007, pp. 493–96.
53. A. Ishmurzin: Ph.D. Thesis, University of Leoben, Austria, 2009.
54. L. Könözsy, F. Mayer, A. Ishmurzin, M. Wu, A. Ludwig, R. Tanzer, and W. Schützenhöfer: *2nd International Conference on Simulation and Modeling in Metallurgical Processes in Steelmaking*, A. Ludwig, ed., Graz, Austria, 2007, pp. 126–32.
55. J. Campbell: in *Castings*, Butterworth Heinemann Ltd., Oxford, U.K., 1991, pp. 151–58.
56. M. Bellet, H. Combeau, Y. Fautrelle, D. Gobin, M. Rady, E. Arquis, O. Budenkova, B. Dussoubs, Y. Duterrail, A. Kumar, C.A. Gandin, B. Goyeau, S. Mosbah, and M. Založnik: *Int. J. Therm. Sci*., 2009, vol. 48, pp. 2013–16.
57. N. Ahmad, H. Combeau, J. Desbiolles, T. Jaldanti, G. Lesoult, J. Rappaz, M. Rappaz, and C. Stomp: *Metall. Mater. Trans. A*, 1998, vol. 29A, pp. 617–30.
58. P. Roux, B. Goyeaau, D. Gobin, F. Fichot, and M. Quintard: *Int. J. Heat Mass Trans*., 2006, vol. 49, pp. 4496–4510.
59. J. Li, M. Wu, J. Hao, and A. Ludwig: *Comp. Mater. Sci*., 2012, vol. 55, pp. 407–18.
60. J. Li, M. Wu, J. Hao, A. Kharicha, and A. Ludwig: *Compt. Mater. Sci*., 2012, vol. 55, pp. 419–29.
61. D.J. Hebditch and J.D. Hunt: *Metall. Trans*., 1974, vol. 5, pp. 1557–64.
62. L. Könözsy, A. Ishmurzin, F. Mayer, M. Grasser, M. Wu, and A. Ludwig: *Int. J. Cast Metals Res*., 2009, vol. 22, pp. 175–78.
63. R. Tanzer, W. Schützenhöfer, G. Reiter, H.-P. Fauland, L. Könözsy, A. Ishmurzin, M. Wu, and A. Luwig: *International Symposium on Liquid Metal Processing and Casting*, P.D. Lee *et al*., eds., Nancy, France, 2007, pp. 121–26.
64. R. Tanzer, W. Schützenhöfer, G. Reiter, H.P. Fauland, L. Könözsy, A. Ishmurzin, M. Wu, and A. Ludwig: *Metall. Mater. Trans. B*, 2009, vol. 40B, pp. 305–11.
65. M. Wu and A. Ludwig: *Acta Mater*., 2009, vol. 57, pp. 5621–31.
66. M. Wu and A. Ludwig: *Acta Mater*., 2009, vol. 57, pp. 5632–44.
67. M. Wu and A. Ludwig: *Int. J. Cast Metals Res*., 2009, vol. 22, pp. 323–27.
68. M. Wu and A. Ludwig: *12th International Conference on Modeling of Casting, Welding, Advanced Solidification Processes*, S.L. Cockcroft *et al*., eds., Vancouver, Canada, 2009, pp. 537–44.
69. M. Wu, A. Fjeld, and A. Ludwig: *Compt. Mater. Sci*., 2010, vol. 50, pp. 32–42.
70. M. Wu, A. Ludwig, and A. Fjeld: *Compt. Mater. Sci*., 2010, vol. 50, pp. 43–58.
71. M. Wu, L. Könözsy, A. Ludwig, W. Schützenhöfer, and R. Tanzer: *Steel Res. Int*., 2008, vol. 79, pp. 637–44.
72. L. Könözsy, A. Ishmurzin, M. Grasser, M. Wu, A. Ludwig, R. Tanzer, and W. Schützenhöfer: *Mater. Sci. Forum*, 2010, vol. 649, pp. 349–54.
73. D.K. Melgaard, R.L. Williamson, and J.J. Beaman: *JOM*, 1998, vol. 50, pp. 13–17.
74. B. Hernandez-Morales and A. Mitchell: *Ironmak. Steelmak*., 1999, vol. 26, pp. 423–438.
75. V. Weber, A. Jardy, B. Dussoubs, D. Ablitzer, S. Rybéron, V. Schmitt, S. Hans, and H. Poisson: *Metall. Mater. Trans. B*, 2009, vol. 14B, pp. 271–80.
76. A. Kharicha, W. Schützenhöfer, A. Ludwig, R. Tanzer, and M. Wu: *Int. J. Cast Metals Res*., 2009, vol. 22, pp. 155–59.
77. A. Kharicha, W. Schützenhöfer, A. Ludwig, and R. Tanzer: *Steel Res. Int*., 2008, vol. 79, pp. 632–36.
78. A. Kharicha, W. Schützenhöfer, A. Ludwig, R. Tanzer, and M. Wu: *2nd Internatinal Conference on Simulation & Modeling of Metallurgical Processes in Steelmaking*, A. Ludwig, ed., Graz, Austria, 2007, pp. 105–10.
79. A. Kharicha, A. Mackenbrock, A. Ludwig, W. Schützenhöfer, V. Maronnier, M. Wu, and O. Köser: *International Symposium on Liquid Metal Processing and Casting*, P.D. Lee, A. Mitchell, J.P. Bellot, A. Jardy, eds., Nancy, France, 2007, pp. 107–13.
80. A. Kharicha, A. Mackenbrock, A. Ludwig, W. Schützenhöfer, V. Maronnier, M. Wu, O. Köser, and R. Tanzer: *International Symposium on Liquid Metal Processing and Casting*, P.D. Lee, A. Mitchell, J.P. Bellot, A. Jardy, eds., Nancy, France, 2007, pp. 113–19.
81. A. Kharicha, A. Ludwig, and M. Wu: *Mater. Sci. Eng. A*, 2005, vol. 413, pp. 129–34.
82. A. Kharicha, W. Schützenhöfer, A. Ludwig, and G. Reiter: *Mater. Sci. Forum*, 2010, vol. 649, pp. 229–36.
83. A. Kharicha, A. Ludwig, and M. Wu: *International Symposium on Liquid Metal Processing and Casting*, M.J.M. Krane, R.L. Williamson, J.P. Bellot, A. Jardy, eds., Nancy, France, 2011, pp. 113–19.
84. A. Kharicha, A. Ludwig, and M. Wu: *4th International Conference on Simulation and Modeling in Metallurgical Processes in Steelmaking*, Düsseldorf, Germany, 2011, pp. S19.1–5.
85. G. Chirita, I. Stefanescu, J. Barbosa, H. Puga, D. Soares, and F.S. Silva: *Int. J. Cast Metals Res*., 2009, vol. 22, pp. 382–89.
86. G. Chirita, I. Stefanescu, D. Soares, and F.S. Silva: *Anales de Mecánica de la Fractura*, 2006, vol. 23, pp. 317–22.
87. K.S. Keerthi Prasad, M.S. Murali, P.G. Mukunda, and S. Majumdar: *Met. Mater. Trans. B*, 2010, vol. 42B, pp. 144–55.
88. P. Raju and S.P. Mehrotra: *Mater. Trans. JIM*, 2000, vol. 41, pp. 1626–35.
89. Z. Xu, N. Song, R.V. Tol, Y. Luan, and D. Li: *Mater. Sci. Eng*., 2012, vol. 33, pp. 1–8.
90. E. Kaschnitz: *Mater. Sci. Eng*., 2012, vol. 33, pp. 1–6.
91. S.R. Chang, J.M. Kim, and C.P. Hong: *ISIJ Int*., 2001, vol. 41, pp. 738–47.
92. K.S. Keerthi Prasad, M.S. Murali, P.G. Mukunda, and S. Majumdar: *Metall. Mater. Trans. B*, 2010, vol. 42B, pp. 144–55.
93. P.S.S. Raju and S.P. Mehrotra: *JIM*, 2000, vol. 41, pp. 1626–35.